

Heat pump enhanced heat recovery from flue gas of wood chips combustion

Babette Hebenstreit^{ab}, Manuel Schwabl^c, Ernst Höftberger^d, Bernhard Kronberger^e, Bernd Gappmayer^f, Hermann Gautsch^g, Joakim Lundgren^h, Andrea Toffoloⁱ

^a BIOENERGY 2020+ GmbH, Gewerbepark Haag 3, 3250 Wieselburg-Land, Austria, CA, babette.hebenstreit@bioenergy2020.eu

^b Luleå University of Technology, SE-971 87 Luleå, Sweden

^c BIOENERGY 2020+ GmbH, ernst.hoefberger@bioenergy2020.eu

^d BIOENERGY 2020+ GmbH, manuel.schwabl@bioenergy2020.eu

^e VOIGT+WIPP Engineers GmbH, Märzstraße 120, 1150 Wien, Austria, kronberger@voigt-wipp.com

^f Fernwärmeversorgungs-GmbH Tamsweg, Wölting 74, Austria, fhw@sbq.at

^g Frigopol Energieanlagen GmbH, 8523 Frauental, Austria, info@gh-energieberatung.com

^h Luleå University of Technology, SE-971 87 Luleå, Sweden, joakim.lundgren@ltu.se

ⁱ Luleå University of Technology, SE-971 87 Luleå, Sweden, andrea.toffolo@ltu.se

Biomass based district heating plants are common in Austria. In 2011, biomass accounted for 46% of the heat produced in Austrian district heating systems. The biomass source is mostly wood chips with water contents in the range of 30-60%, leading to a high water vapour content in the flue gas. A condensing heat exchanger operating at temperatures below the water dew point of the flue gas is necessary to recover the latent heat of the water vapour. This heat is often unused because of a missing low temperature heat sink. One possibility to overcome this issue is to use a heat pump, which provides the low temperature heat sink and transfers the heat energy to higher temperatures. This concept is called active condensation.

In 2012, an active condensation system was installed in a biomass heating plant in Austria. In the paper the data from a measurement campaign about plant operation with and without heat pump are compared to deduce the heat recovery rate and the corrosion potential. The results indicate that a different hydraulic connection, in which the heat pump condenser operates at a higher temperature level, should improve both the heat recovery and the corrosion potential.

Keywords: Biomass, Flue gas condensation, Heating plant, Heat pump, Waste heat recovery.

1 Nomenclature

CHEX	flue gas condensing heat exchanger
CON	condenser (of HP or ORC cycle)
DH	district heating
ECO	thermal oil-water economizer
el	electric
EVA	evaporator
HEX	heat exchanger
HP	heat pump
HT	high temperature return flow
LT	low temperature return flow
ORC	organic rankine cycle
\dot{Q}	thermal power
P	electric power
T	temperature
th	thermal

2 Introduction

The amount of biomass used for district heating is increasing steadily in Austria, from 10.4 PJ of delivered heat in 2005 to 31.1 PJ in 2011 (a 46% share of the thermal energy delivered in Austrian district heating networks) [1]. Biomass is mostly used in small and medium sized boilers. 1.140 biomass boilers with a nominal load of minimum 1 MW are installed in Austria [2], and they sum up to a nominal load of about 3.000 MW.

Since the energy from biomass is limited it is necessary to gain a high rate between the delivered heat and the fuel spent to generate it. Although state of the art boilers are able to make available 90-97% of the net calorific value of the fuel, there is still potential to enhance this rate for most systems. The main heat losses are flue gas losses and distribution losses in the heating grid. This paper focuses on heat recovery of the latent heat from flue gas, since biomass with a high water content, as between 30% and 60% in fresh woodchips, leads to a high water content in the combustion products. However, the latent heat stored in the water vapour is only available at temperatures below the water dew point of the flue gas, while in typical district heating applications the return water temperature is almost in the same range (around 50-70°C).

One option to increase the heat output of the system for a given fuel input is the application of a heat pump to create a low temperature sink for the latent heat of the water vapour, and this concept is called "active condensation". Different heat pump concepts like thermal or compression type heat pumps can be applied. The main advantages of compression heat pumps are the lower investment costs as well as the wider range of applications already on the market, while the drawback is the usage of electricity as primary energy input. Thus, a detailed evaluation of the concept is necessary to determine useful application areas. The implementation of compression heat pumps was already discussed for different plants [3-6]. However, these papers focus on the design at nominal load. To the knowledge of the authors no monitoring data has been published.

This study discusses real world operating data of an active condensation system at a heating plant in Austria. Detailed results from the measurement campaign at the demonstration plant are presented and compared to the reference case without active condensation. The analysis of the measurements at different temperature set points for the heat pump and of the corrosion potential should offer indications about how to operate the heat pump in order to obtain a high heat recovery rate, a low electric consumption, and a low corrosion risk. Furthermore the heat transfer coefficients in the condensing heat exchanger are evaluated to assist future implementations of condensation systems at other plants.

3 Material and methods

3.1 Plant description

Figure 1 shows a sketch of the heating plant, which contains two boilers (5 + 3 MW_{th} nominal load). The heat from the 5 MW_{th} one is directly supplied to the district heating water circuit. The heat from the 3 MW_{th} boiler feeds an organic rankine cycle (ORC) with a nominal electric load of 0.52 MW_{el}. The ORC condenser and the flue gas economizer (ECO) also release heat to the district heating, providing the base load thermal output. In fact, the ORC is operated during the whole year, while the 5 MW furnace is only used during the heating season and adapted to the actual heat demand. Furthermore, during the heating season the flue gas of both boilers is mixed and directed to a condensing heat exchanger (CHEX). The heat gained in the condensing heat exchanger is used for preheating the return flow.

Figure 2 shows the hydraulics of the heating plant. The district heating system has two return flows, the main one being at a higher temperature (HT) and the other (approximately 20% of the flow) is collected in a separate pipe at a lower temperature (LT). The condensing heat exchanger contains six tube bundles. The flue gas flows on the outer side from the top to the bottom while the water flows in the tubes. Each tube bundle consists of a matrix of 40 x 8 tubes with an inner diameter of 18 mm and a wall thickness of 1 mm.

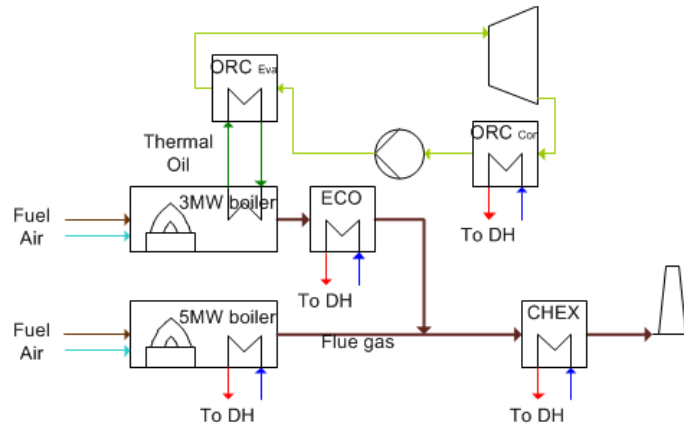


Figure 1: Simplified sketch of the plant. DH – district heating, ORC – Organic Rankine Cycle, CHEX – condensing heat exchanger, ECO – economizer.

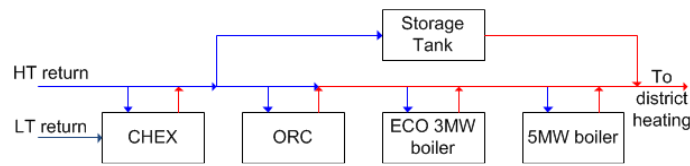


Figure 2: Sketch of the plant hydraulics. ORC – Organic Rankine Cycle, ECO – economizer

3.2 Integration of the heat pump

A heat pump is integrated into the heating plant to increase the condensation of the flue gas occurring in the condensing heat exchanger. Figure 4 shows the hydraulic connections of the tube bundles of the condensing heat exchanger before and after the heat pump integration. The six tube bundles are grouped for sake of simplicity into three sub heat exchangers (HEX1, HEX2 and HEX3) containing one, two, and three bundles respectively. In the reference case without active condensation the bundles simply operate in series, with the exception of the bundle at the lowest temperature (HEX1) which is devoted to increase the temperature of LT return flow before it is mixed with the HT return flow.

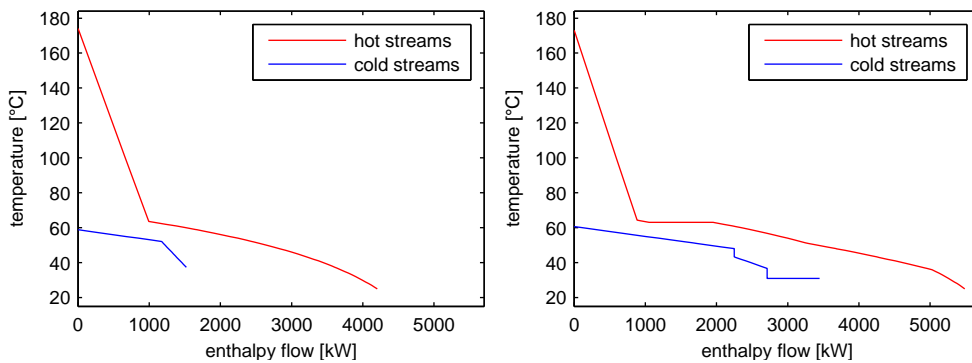


Figure 3: Pinch diagram of CHEX a) without heat pump; b) with heat pump.

An analysis of the flue gas leaving the condensing heat exchanger shows that a large amount of heat is available in the temperature region between 25 and 50°C, which is not utilized. Figure 3a gives the pinch diagram of the enthalpy streams in flue gas and return flows at the reference case. Figure 3b indicates, that a heat pump with a thermal power of 900 kW can be integrated (according to the scheme in Figure 4) to enhance the heat recovery.

However, because of space constraints no additional heat exchanger surface could be added and therefore the hydraulics of the available condensing heat exchanger was changed to integrate the heat pump. In the active condensation case the heat pump uses part of the HT return flow as heat source for the evaporator (HP_{EVA}). The heat pump condenser (HP_{CON}) uses the total return flow as

heat sink at a higher temperature. Thus, the heat pump operates on the side of the return flow only with a net thermal power released to the return flow that is equal to the electric input:

$$\dot{Q}_{HP} = \dot{Q}_{HPCON} - \dot{Q}_{HPEVA} = P_{HPel} \quad (1)$$

At the same time the heat pump indirectly increases the thermal power transferred in the condensing heat exchanger mainly by increasing the water mass flow rate in HEX1 and lowering the water temperature in HEX2.

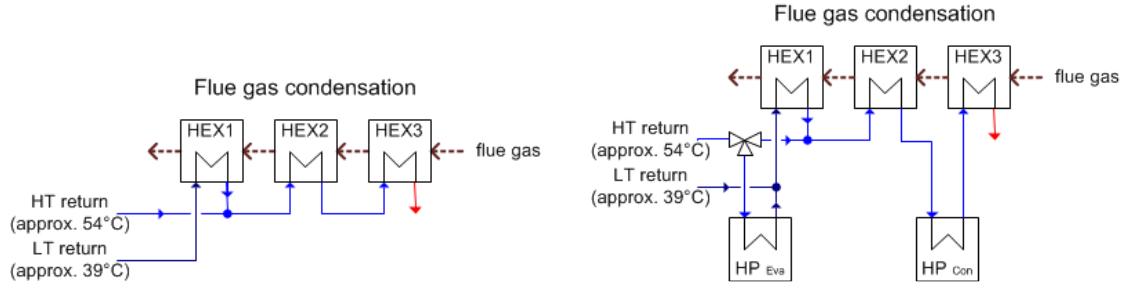


Figure 4: Sketch of the condensation system before (left) and after (right) the integration of the heat pump.

In fact, the water exiting the heat pump evaporator is mixed (almost isothermally) with the LT return flow before entering HEX1. This strongly increases the water mass flow in HEX1 and thus the thermal power transferred in the bundle. The water entering HEX2 has also a slightly lower temperature level than the HT return flow from the district heating. In the current active condensation layout HEX3 is fed with the heated water coming from the outlet of the heat pump condenser. This may not be the most convenient temperature range for the heat pump sink, which should be the result of a compromise between the objectives of lowering the temperatures of the water side in the condensing heat exchanger as much as possible and of keeping the electric input of the heat pump as low as possible. Probably a different distribution of the bundles between HEX2 and HEX3 would be more beneficial in this sense. With the current configuration, HEX1 and HEX2 work most of the time in condensing mode, but HEX3 works either in condensing or non-condensing mode, depending on the water temperature and the water dew temperature of the flue gas.

3.3 Measurement setup and data evaluation

Table 1: Measurement points

Measurement points	Sensor	Estimated Error	Sampling rate
HEX2+HEX3+HP _{CON} , HP _{CON} , HP _{EVA} , HT, LT, Boiler1, ORC, ECO,	Heat meter (temperature, volume flow, thermal power)	1°C, 1 m ³ /h, 10 kW, min 10%	120 s
Water temperatures: Bundle 4-6 In, Bundle 6 Out, HP in/out, NT/HT return	Pt100 or Pt1000	0.5°C	1 s
Flue gas humidity	Combined monolithic relative humidity/ temperature cell	(1.5 + 1.5%*mv) % RH, 1°C	1 s
Flue gas temperature: Between each bundle	Thermocouple Typ K	5°C	1 s
Absolute pressure flue gas: At bundle 4	Pressure transducer	1%	1 s
O ₂ in flue gas	Gas analyzer: electrochemical cell	0.2%abs	1 s
Dynamic pressure in flue gas	Four Prandtl pipes + pressure transducer	5%	1 s
Condensate	Manual reading from meter, pump works discontinuously	0.1 kg/s	15 min

The permanently installed equipment of the plant was used for the measurements. To monitor the plant all heat producers (both boilers, ECO, heat pump, CHEX) are equipped with heat meters. Additional sensors were installed in the condensing heat exchanger to measure the flue gas

temperatures, selected water temperatures, humidity of the flue gas and absolute pressure. All measurement points are listed in Table 1. All measurement values were averaged to 15 min interval data.

Relevant quantities related to the condensing heat exchanger were calculated both on the water and gas sides. On the water side it is possible to calculate the thermal power transferred in HEX1, HEX2 and HEX3 through simple energy and mass balances. On the flue gas side the water dew point temperature and pressure are calculated with the Antoine equation using the relative humidity and absolute pressure. The flue gas volume flow is calculated from the measured dynamic pressure in the flue gas flow at the CHEX inlet assuming ideal gas conditions.

Measurements from the elemental analysis of the fuel, the grate ash, the electrostatic precipitator ash and the condensate were used to reconstruct the balance of the single chemical elements. The ashes were weighted over the measurement period and the associated mass flows were calculated. The mass flows of the fuel and the flue gas were calculated from an energy balance of the measured thermal load in the boiler heat meters.

4 Results

4.1 Energy balance with and without heat pump

In January 2014, a measurement campaign for five operating condition cases was performed at the heating plant, one case being the reference case without the heat pump and the other four cases featuring the heat pump working at different operating points. In order to obtain stable load conditions, the volume flows through the boilers were fixed and the experimental data were recorded for a period of four hours in each of the five cases.

Table 2: Operating conditions in the five cases of the measurement campaign

Short name	Heat pump operating	Water temperature at heat pump evaporator outlet [°C]	5MW boiler pump speed [%]	Additional information
RefH	No	-	70	Reference case
HP38H	Yes	38	70	Measurement duration only 2.5 h, some sensors are missing
HP36H	Yes	36	70	
HP38L	Yes	38	55	
HP34L	Yes	34	55	

Table 2 describes the different operating conditions of the cases. The four cases operating with active condensation are designated according to the overall thermal load requested to the plant (high or low, hence the letter H or L at the end of the short name of the case and the difference in the speed of the 5MW boiler pump) and to the temperature of the water at the heat pump evaporator outlet (a lower temperature corresponds to a lower mass flow rate taken from the HT return flow since the heat pump is supposed to operate at full load).

Figure 5a shows the averaged power outputs from the plant in each case. There are five thermal power outputs: from the 5MW boiler, the ORC condenser, the economizer, the condensing heat exchanger and, in active condensation cases, the heat pump (according to the hydraulic connection shown in Figure 4 the net thermal power flow from the heat pump to the district heating water equals the electric power input to the heat pump itself). The electric power output from the ORC is also shown. It is apparent that in active condensation cases the share of the condensing heat exchanger output is increased, in particular in the cases with lower overall plant loads.

A detailed analysis of what happens in the bundle groups of the condensing heat exchanger is offered in Figure 5b. It shows that the insertion of the heat pump according to the scheme in Figure 4 makes the thermal powers transferred in groups HEX1 and HEX2 increase, while that in group HEX3 decreases. This is due to the higher water mass flow in HEX1 and the lower water inlet temperature in HEX2, as already expected according to the comments to Figure 4. On the contrary, the water inlet

temperature in HEX3 gets higher because of the heat released by the heat pump condenser just upstream the group inlet.

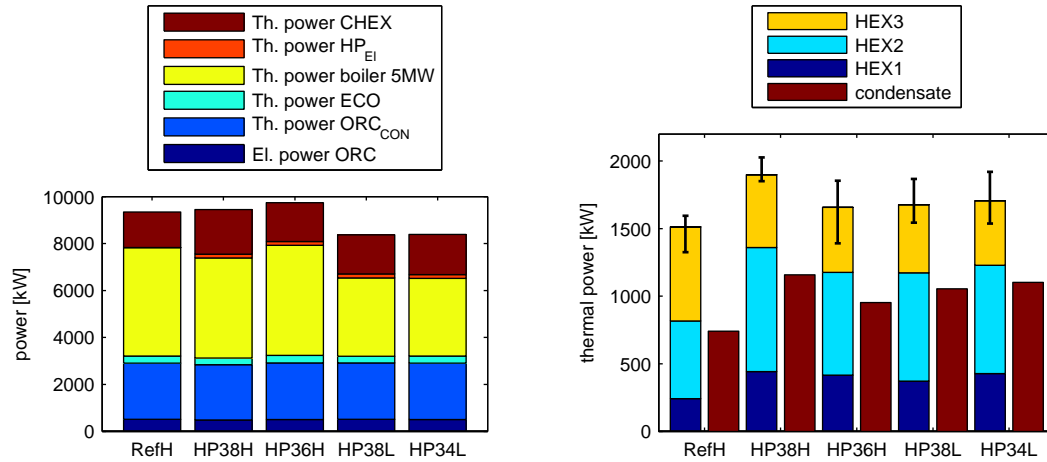


Figure 5: a) Thermal and electric power outputs of the plant. b) Thermal power in the bundle groups of the condensing heat exchanger (HEX1, HEX2 and HEX3) and thermal power associated with flue gas condensation.

In the same figure, the thermal power associated with the condensate is shown as a separate bar. This is calculated as the product of the condensate mass flow (which is measured) and the latent heat of water at an arbitrary reference temperature (50°C) chosen inside the condensation temperature range. The comparison among the cases shows that the exploitation of the latent heat on the flue gas side is increased by active condensation. The increase in the amount of condensed water is between 28% and 56% compared to the reference case (see Table 3).

Table 3: Results of active condensation cases compared with reference case. The values with * are compared to RefH although the 5MW boiler power was lower. The value n.a. are not available due to missing measurement.

	RefH	HP38H	HP36H	HP38L	HP34L
Average over 4h					
Electric power HP [kW]	-	168	162	166	157
Thermal power CHEX [kW]	1512	1898	1656	1664	1707
Condensation rate [kg/s]	0.31	0.49	0.40	0.44	0.46
Increase compared to RefH [%]	-	56	28	42*	49*
Selected 15min sets with lowest difference in external conditions compared to RefH					
Plant power (th+el) [kW]	9382	9418	10107	8347	7950
Electric power HP [kW]	-	167	164	165	161
Thermal power CHEX [kW]	1534	1852	1802	1728	1578
CHEX effectiveness	0.43	n.a.	0.54	0.62	0.50
Active condensation ratio	-	2.90	2.63	2.17*	1.27*

However, the heat transferred in the condensing heat exchanger is strongly influenced by the fluctuations of the “real world” operating conditions during the measurement period. This is indicated by the error bars in Figure 5b, which show the measured minimum and maximum average values in the 15 minutes intervals in which the whole 4h measurement period was divided. For instance, the volume flow and temperature of the return flows change, and so does the dew point in the flue gas as a function of the fuel water content and the combustion air ratio. Figure 6 show 15 minutes average data of temperatures and power. It can be noted that the LT return temperature varies strongly and influences the thermal power of HEX1, especially in the reference case. Moreover, the figures show that the thermal power of HEX2 correlates with the dew temperature of the flue gas.

For each case one 15 minutes average data set was selected (identified with the mark in Figure 6 among the data for whole 4 hour period), in order to have the smallest difference in the external uncontrolled conditions with the reference case. The selected sets and the reference case lie in a

range of 3 K for the LT and HT return temperatures, 0.5 kg/s for the LT volume flow, 1.3 kg/s for the HT volume flow, and 2 K for the flue gas water dew temperature. These selected sets were used for further evaluations with the results shown in Table 3.

The desired effect of the heat pump installation is to increase the amount of heat recovered in the condensing heat exchanger and to transfer it to the district heating return flow. Two indices can be defined to quantify at a glance the outcome of this operation. The first one, named CHEX effectiveness, is defined as the ratio between the thermal power transferred in the condensing heat exchanger and the reference thermal power that could be transferred in the same heat exchanger if the flue gas could be cooled down to the temperature of LT return flow and the water vapour condensed according to the corresponding saturation conditions.

$$\frac{\dot{Q}_{\text{CHEX}}}{\dot{Q}_{\text{CHEX,max}}|_{T_{\text{LT}}}} \quad (2)$$

On the other hand, the second one, named active condensation ratio, is defined as the ratio between the additional heat gained in the active condensation case by the district heating water and the amount of energy that has been spent to make that happen, i.e. the electric input of the heat pump:

$$\frac{\dot{Q}_{\text{CHEX}} + P_{\text{HPel}} - \dot{Q}_{\text{CHEX,Ref}}}{P_{\text{HPel}}} \quad (3)$$

The numerator is equal to the difference between the heat transferred in the condensing heat exchanger in the active condensation case and in the reference case plus the electric input of the heat pump, which is the only net contribution of the heat pump to the district heating water according to the hydraulic connections in Figure 4. This ratio is also similar to a coefficient of performance used in heat pumping technology and corresponds to the amount of heat (additional heat in this case) per electric input. Table 3 shows that CHEX effectiveness increases from 0.43 at the reference case to values between 0.50 and 0.62 with the heat pump. The active condensation ratio is calculated to values between 2.63 and 2.90 for the high load cases. The values for the low load cases (1.27 and 2.17) are lower because the high load reference point is used in the calculation.

The cases with higher evaporator outlet temperature (HP38H and HP38L) lead to a higher CHEX effectiveness as well as a higher active condensation ratio than the cases with the same load but lower evaporator outlet temperature (HP36H and HP34L). Thus, in the current hydraulic connection the evaporator outlet temperature of 38°C is preferable.

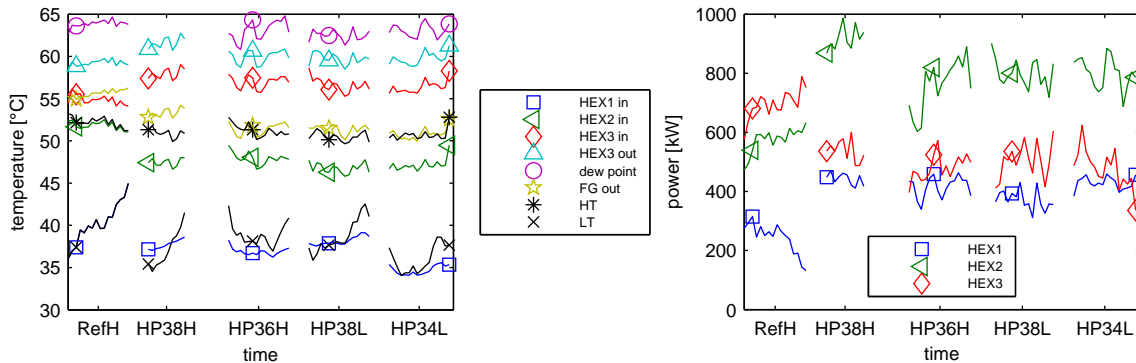


Figure 6: a) Temperatures in the condensing heat exchanger. b) Thermal power in the condensing heat exchanger.

4.2 Mass balance of chemical elements

A mass balance of chemical elements was conducted to investigate the corrosion potential, i.e. to assess the concentration of acidic compounds of corrosive elements like chlorine and sulphur in the condensate. In fact, the presence of the corrosive chemical elements in the condensate can have two origins. On the one hand, some of them are dissolved from the gaseous phase and form a high concentrated acidic solution. On the other hand, some are bound with particulate matter that gets trapped in the condensate, but in this case their deposition on the heat exchanger surface in the form

of salts have a different corrosion mechanism. As a consequence the two different origins are distinguished in the chemical element balances. This was done as in [7] by measuring the composition of the filter ash as well. The composition of the ashes (which should reflect the composition of the particulate matter) was then compared with the concentration of the species in the condensate. Since the only origin of potassium in the condensate is the trapped particulate matter, the ratio in the condensate between the chlorine and sulphur from trapped particulate matter and potassium must be the same as in the ash composition, so the corresponding amounts of the corrosive elements are subtracted to the concentration found in the condensate analysis to determine their corrosive potential.

Figure 7a shows the average mass of the inorganic elements found in the fuel. The main share of these masses is collected in the ash, while only a small amount is found in the condensate. However, chlorine and sulphur were recovered to 7 and 38% in the condensate. Figure 7b shows the mass of the elements found in the condensate and their origin (dissolved gaseous phase or trapped particulate matter). It indicates that large amounts of both sulphur and chlorine are dissolved from the gaseous phase, originating from gaseous acidic compounds like HCl, SO₂ and SO₃.

Therefore, in order to avoid a highly concentrated acidic solution on the surface of the condensing heat exchanger, it must be guaranteed that there is always a sufficient water film to protect the surface. This means that the temperature of the surface of the heat exchanger should always be lower than the water dew temperature, since the acidic compounds have a higher dew temperature than that of water. According to the measurements performed, the water dew point of the flue gas was always higher than the temperatures on the water side of all bundles (see Figure 6), and that should be sufficient to guarantee that the temperature of the heat exchanger surface on the flue gas side is always lower than the water dew temperature.

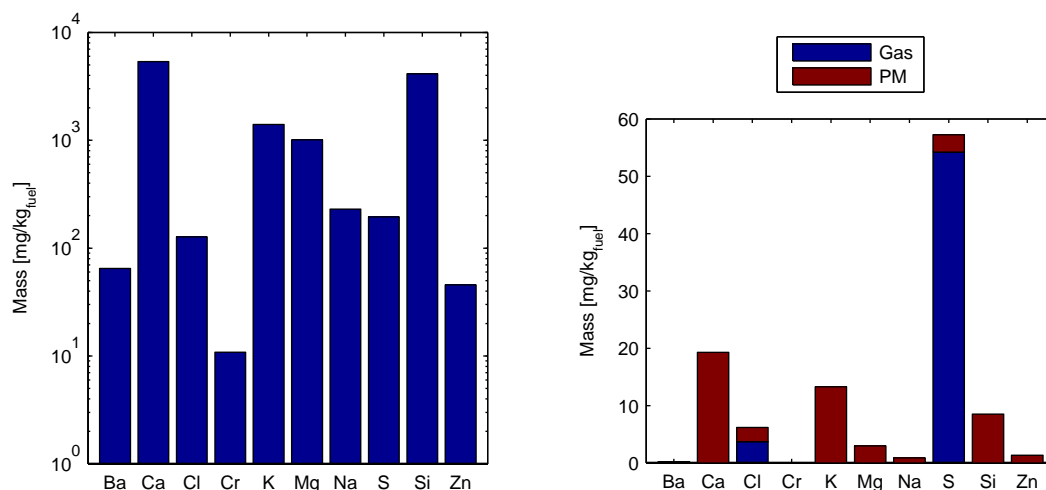


Figure 7: Mass balance of chemical elements. a) Total amount per kg fuel. b) Mass of chemical elements found in condensate from gaseous source (Gas) and from particulate matter (PM).

However, the dew point temperature is usually lower in other operating conditions that were not considered in the measurement campaign, such as at low boiler power with higher air ratios or for a fuel with a lower water content. In this case high concentration acidic solution is likely to form on the surface leading to corrosion. Thus, keeping the water temperature low in the HEX3 group of bundles is critical in order to avoid corrosion on the heat exchanger surface. This means that the temperature range at which the heat from the heat pump condenser is released plays an important role in the corrosion, and connecting the heat pump condenser after all the bundles of the condensing heat exchanger would be the most preferable solution to reduce the risk of corrosion.

The corrosion potential of the particulate matter deposits on the heat exchanger is strongly dependent on the hygroscopic effect of the particulate matter, which was not directly investigated within this work. However, this effect allows corrosion even when the relative humidity at the heat exchanger surface is below 50%. According to tables for the deliquescence of pure salts [8], potassium hydroxides and carbonates are highly hygroscopic salts. Considering the elemental composition of the particulate matter, carbonates, hydroxides and oxides are very likely to exist in this system, which are increasing

the effective corrosion dew temperature of the system. This corrosive effect can be avoided, when the deposits are continuously washed off the heat exchanger surface.

4.3 Condensing heat transfer rates

A detailed investigation of the heat transfer rates in the bundles of the condensing heat exchanger is carried out to generalize the results for other heating plants. The pressure difference between the steam partial pressure in the flue gas and the saturation pressure on the bundle surface is the driving force of the condensation rate. If this pressure difference is negative, no condensation can occur.

Among the set of measurements that were performed, the relative humidity in the flue gas at HEX3 bundle group and the temperature of the water in the bundles are used to calculate the steam pressure in the flue gas and the water saturation pressure on the bundle surface, respectively, in order to approximate the driving force of condensation with their difference. Figure 8a shows the heat transfer coefficient vs. this difference. At a pressure difference of approximately 5000 Pa a bend occurs, indicating the limit between the non-condensing and the condensing regimes. The heat transfer coefficient is between 20 and 70 $\text{W/m}^2\text{K}$ in the non-condensing regime, while in the condensing regime it rises strongly reaching a maximum of about 400 $\text{W/m}^2\text{K}$. Figure 8b shows the heat transfer coefficient for 15 min average data in a period of 10 days displaying a much larger variety of operating conditions.

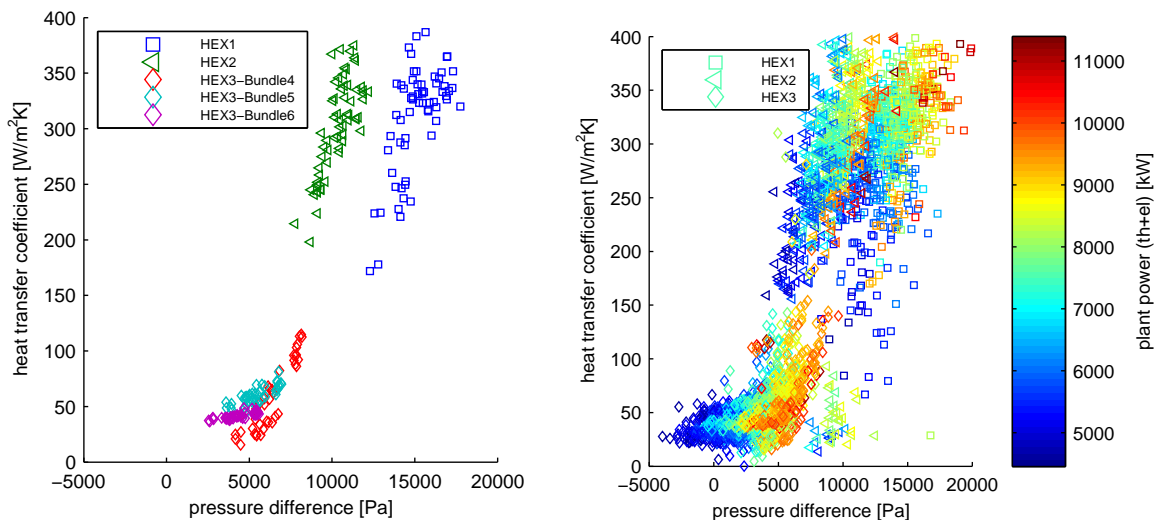


Figure 8: Heat transfer rate in the condensing heat exchanger vs. the approximated pressure difference driving the condensation. a) Data from operating points in Table 2. b) Data registered between 26.1.2014 and 5.2.2014, the colour indicates the plant power (thermal and electric outputs).

In these two figures, the abscissas of the values for the different bundle groups seem to be mismatched (e.g., those for HEX1 seem to be shifted to the right by about 3000 Pa with respect to those for HEX2). This is due to the way in which the pressure difference is approximated since the same measurement of relative humidity taken on the flue gas side of HEX3 is actually used for all the bundles. In reality, the steam partial pressure is expected to continuously drop from the top (HEX3) to the bottom (HEX1) of the condensing heat exchanger because of the condensation. Therefore, the approximated pressure difference used in the figure is systematically higher than the real pressure difference.

5 Conclusions and outlook

A heat pump was integrated into the condensing heat exchanger of a heating plant fired with wood chips. The heat pump was tested with different evaporator outlet set points and at two different plant thermal loads (in total four active condensation cases and one reference case without heat pump). In the active condensation cases the condensing heat exchanger effectiveness was between 0.50 and 0.62 compared to 0.43 in the reference case. The measured thermal output of the condensing heat exchanger increased by approx. 300 kW compared to the reference case at the high load cases,

corresponding to an active condensation ratio of 2.63 to 2.90. The higher thermal output of the condensing heat exchanger is also reflected in the increase of condensed water between 28 to 56 % compared to the reference case. The calculated heat transfer coefficients are between 20 and 70 W/m²K in the non-condensing regime and up to 400 W/m²K in the condensing regime.

The measurements showed a decrease of the thermal power in bundle group HEX3 compared to the reference case. For the future it is suggested to change the hydraulic integration of the heat pump condenser at a higher temperature level. Since this will result in a lower coefficient of performance of the heat pump, a compromise between a higher thermal power in the condensing heat exchanger and a lower coefficient of performance should be selected.

For the current hydraulic connection the evaporator outlet temperature set point of 38°C is preferable to the lower temperature set point. However, the choice of the best operating point of the heat pump evaporator temperature varies with the fluctuations of the dew point and the temperatures of the return flow. Therefore, the development of a mathematical model of the condensing heat exchanger is planned in the future. Its simulation will help to determine the best operating point and to develop a control strategy for the heat pump set points depending on boiler power and return flow temperatures. As a basis for the model the evaluated heat transfer coefficients can be used.

Furthermore the corrosion potential should be considered in the control strategy. The mass balance of the chemical elements in the heating plant showed that both sulphur and chlorine are mostly dissolved from the gaseous phase. Therefore, the temperature on all bundle surfaces should always be kept below the water dew point.

6 Acknowledgements

This work was funded within the framework of the NEUE ENERGIEN 2020 (new energies 2020) research program out of the Klima- und Energiefonds (climate and energy fund), Austria and by the province of Salzburg, Austria. Furthermore we thank the Friedrich Schiedel Foundation for Energy Technology for funding the project ActiveCondDyn through which a detailed evaluation of the measurement data was possible. We also like to acknowledge the support of the plant operators (Fernwärmeversorgung-GmbH Tamsweg) and thank the project partners for the excellent collaboration.

7 Bibliography

- [1] Statistik Austria Energiebilanzen 1970-2011. www.statistik.at
- [2] Biermayr, P.; Eberl, M.; Enigl, M.; Fechner, H.; Kristöfel, C.; Leonhartsberger, K.; Maringer, F.; Moidl, S.; Strasser, C.; Weiss, W. & Wörgetter, M. (2014), *Innovative Energietechnologien in Österreich Marktentwicklung 2013. Biomasse, Photovoltaik, Solarthermie, Wärmepumpen und Windkraft. Berichte aus Energie- und Umweltforschung 26/2014*, BMVIT, Wien.
- [3] Chen, Q.; Finney, K.; Li, H.; Zhang, X.; Zhou, J.; Sharifi, V. & Swithenbank, J. (2012), 'Condensing boiler applications in the process industry', *Applied Energy* **89**(1), 30-36.
- [4] Gaderer, M. (2008), 'Wärmeversorgung mit fester Biomasse bei kleiner Leistung', PhD thesis, TU München.
- [5] Hebenstreit, B.; Schnetzinger, R.; Ohnmacht, R.; Höftberger, E.; Lundgren, J.; Haslinger, W. & Toffolo A. (2014), 'Techno-economic study of a heat pump enhanced flue gas heat recovery for biomass boilers', *Biomass and Bioenergy* **71**, 12-22.
- [6] Herrlander, B. (2008), Fuel flexibility and optimal energy recovery requires qualified gas cleaning, in 'Proceedings of the World Bioenergy', pp. 287-292.
- [7] Schwabl, M.; Schmidl, C.; Haslinger, W.; Wopienka, E.; Humel, S.; Voglauer, B. (2011), 'Corrosion relevant properties of flue gas from small scale wooden biofuel combustion' in 'Proceedings of the 19th European Biomass Conference', Berlin.
- [8] Greenspan L. (1977), 'Humidity fixed points of binary saturated aqueous solutions' *Journal of research of the national Bureau of Standards, A. Physics and Chemistry A* **81**, 89-96.